Chapter 3

Theory of Fluidized Bed Combustion

3.1 Principle of Fluidized Bed Combustion

3.1.1 Basic Concept of Fluidization

The fluidization is simple in concept, as shown in Figure 3.1.
If a vertical cylinder of any cross section is closed off at the bottom
with a perforated plate, the cylinder partly filled with a granular
solid material, and sufficient air or gas blown up through the
perforated plate, then the bed of granular material is vigorously
tumbled by the rising bubble and is said to be fluidized. In addition to
having the appearance of a boiling liquid, a fluidized bed exhibits
several properties associated with liquids. It seeks its own level, it
flows through pipes, and it generates a static pressure proportional to
its depth. The velocity at which the bed starts to be fluidized is
called minimum fluidization velocity, U_{mf}.

Additional properties of a fluidized bed are very good mixing
of solids, good mixing of gases and solids, and if a thermal gradient
exists, very good heat transfer. For these reasons, simple fluidized
beds have been used for decades in industry where intimate mixing of
gases and solids is required. Examples are catalytic crackers in
refineries, fluidized bed polymerization in petrochemical processes, and
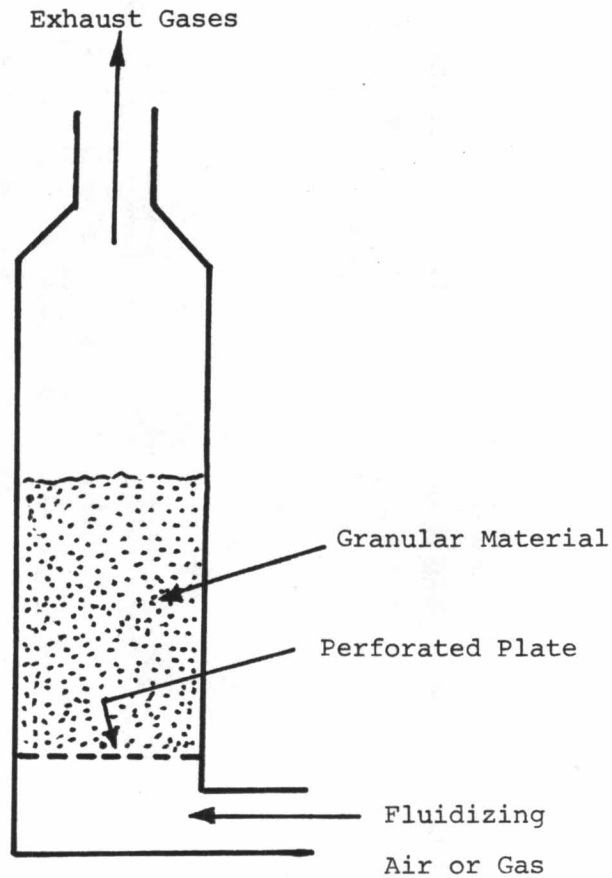some types of ore roasters.[8,9]

Fig. 3.1 An Elementary Fluidized Bed

3.1.2 Fluidized Bed Combustion

Combustion occurring in a state of fluidization is called fluidized bed combustion (FBC). Fluidized bed combustion is a new process with the potential for burning coal and other dirty, sulfur-bearing, fuels in a clean manner and at a cost competitive with conventional combustion methods. In this technique, coal is burned in a fluidized bed of the SO_2 sorbent, typically limestone or dolomite.

At the conditions prevailing in a fluidized bed combustor, limestone and dolemite decompose, or calcine, as shown in the reaction below.

limestone: $CaCO_3 \longrightarrow CaO + CO_2$

dolomite : $CaCO_3 \cdot MgCO_3 \longrightarrow CaO + MgO + 2CO_2$

SO_2 formed in the combustion process is removed down to the required levels by reaction with the sorbent within the combustor as shown in reaction

$$CaO + SO_2 + \tfrac{1}{2} O_2 \longrightarrow CaSO_4$$
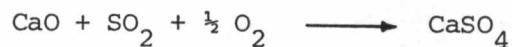
Emissions of nitrogen oxides are also low, due to the low combustion temperature (850 - 950 °C) and   reactions which occur in the fluidized bed and destroy NO_x.

Two basic versions of the fluidized bed combustion process are under development: atmospheric and pressurized. In the pressurized version, pressure in the combustor is usually 6-10 atm. Both the atmospheric and pressured systems each take a number of forms; these forms differ in how the heat energy produced in the combustor is extracted to provide heat elsewhere or to do useful work.

3.1.3 Factors Indicating Fluidized bed Combustor Performance.

There are mainly two factors that indicate fluidized bed combustor performance. To reduce SO_2 and NO_x emissions is the first

factor. The another factor is to burn the char as efficiently as possible, that is the combustion efficiency. The first factor can be performed as mentioned above. Under the limited conditions for reducing emissions, low combustion temperature (850 - 950 °C), a certain mixture ratio of limestone and coal, how to operate to get the maximum combustion efficiency is required. Hence the factors affecting combustion efficiency are considered.

3.2 Combustion Efficiency

The relationship between bed properties, operating conditions, and combustion efficiency is shown in Figure 3.2 .
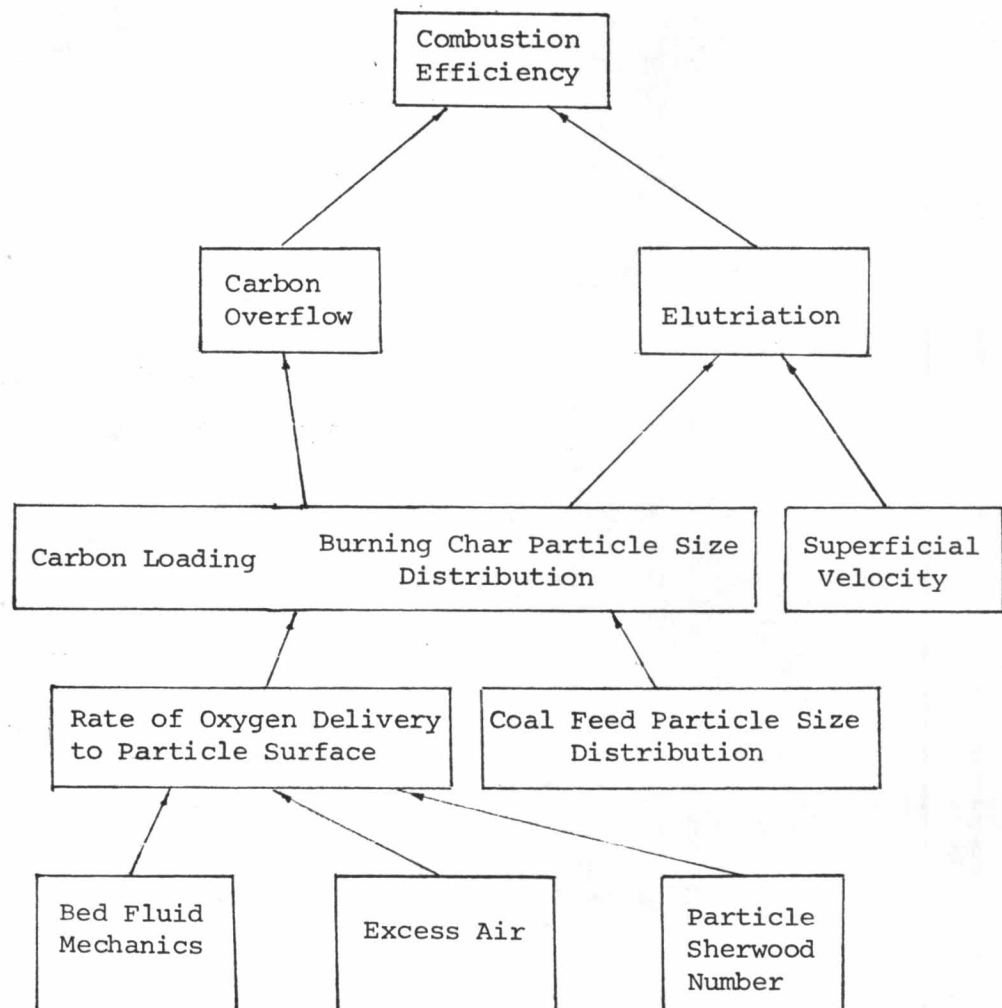
Fig. 3.2 Factors Affecting Combustion Efficiency

Combustion efficiency is inversely proportional to the carbon loss which can occur by two mechanisms: first, via carbon overflow, where the carbon held up in the bed is lost when the spent stone is withdrawn , and second, via elutriation.

The carbon overflow rate depends on carbon loading in the bed. Elutriation is also related to carbon loading as well as the superficial gas velocity and the particle size distribution of carbon in the bed. Thus, a model to predict carbon loading is essential in order to predict combustion efficiency. The structure of such a model is complex. It must account for residence time of burning char particles in bed, the effect of particle shrinkage due to combustion as well as for the critial particle size distribution of the coal feed. The combustion rate or rate of oxygen delivery to the particle surface is itself related to the fluid mechanic characteristics of the bed, the excess air, the particle Sherwood number, and the reaction at the particle surface.

The factors which affect carbon loading are:

(i)   residence time of burning char particles in bed

(ii) gas exchange rate between bubble and dense phase,

(iii) gas exchange rate between dense phase and particle surface, and

(iiii) particle shrinkage rates due to combustion. [10]

3.3 Mass Balance

The mass balance may be determined from consideration of a population balance of carbon feed, carbon burning in bed and elutriation. The model assumes that the solids are well-stirred and the char density is constant while burning. The population balance on the particles is following the notation of Kunii and Levenspiel.[11,12]

Quantitatively, mass balance on the solids in unit time is illustrated by Simple diagram.

$$F_2$$

| Rate of Carbon Combustion in the Bed |

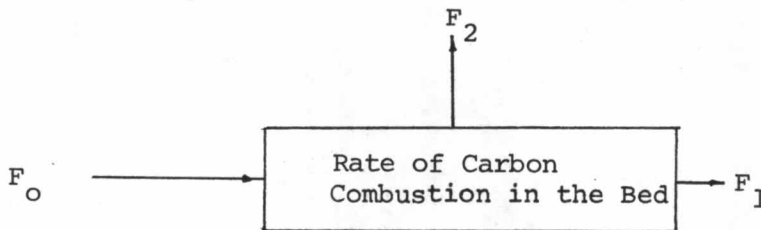$$F_0 \quad\quad\quad F_1$$

Fig. 3.3 Mass Balance Simple Diagram

where F_0 = carbon feed rate

F_1 = carbon overflow rate

F_2 = carbon elutriation rate

The equation can be given by

$F_0 - F_1 - F_2$ = carbon combustion rate in the bed

$$= \sum_{\text{all } R} \left(\begin{array}{l} \text{carbon combustion rate of particles} \\ \text{in the size interval } R \text{ to } R-\Delta R \end{array} \right) \quad \ldots (3.3.1)$$

where R = particle radius

The carbon combustion term accounts for the decrease in size and mass of individual particles due to their shrinkage, and it is found as follows. First the number of particles in the size interval R to $R-\Delta R$ is

$$N(R) = \frac{\text{mass in interval}}{\text{mass / particle}}$$

$$= \frac{W \rho_b (\bar{R}) \Delta R}{\rho_s (\frac{4}{3} \pi \bar{R}^3)} \qquad \ldots \ldots (3.3.2)$$

Where $N(R)$ = the number of particles in the size interval R to $R-\Delta R$

W = total weight of carbon particles in bed

$P_b(\bar{R})$ = particles size distribution of size $\bar{R}$ in bed

$\bar{R}$ = the average size of particle in the interval

ρ_s = density of particle

Then in the time Δt

$$
\begin{pmatrix} \text{mass of carbon combustion} \\ \text{in the size interval} \\ \text{R to R} - \Delta \text{R} \end{pmatrix} = \rho_s \begin{pmatrix} \text{number of particles} \\ \text{in the interval} \end{pmatrix} \begin{pmatrix} \text{volume decrease} \\ \text{of a particle in} \\ \text{time } \Delta t \end{pmatrix}
$$

$$
= \rho_s \left(\frac{WP_b(\bar{R}) \, \Delta R}{\rho_s \frac{4}{3} \pi \bar{R}^3} \right) \left(\frac{-dV}{dt} \cdot \Delta t \right)
$$

Substituting dV by $4 \pi R^2$ dR and letting $\Delta R \longrightarrow$ dR, we find in unit time that

$$
\begin{pmatrix} \text{carbon combustion rate} \\ \text{in the size interval} \end{pmatrix} = \frac{-3WP_b(R) \, \mathscr{R}(R) \, dR}{R} \quad \ldots\ldots\ldots (3.3.3)
$$

where $\mathscr{R}(R) = \dfrac{dR}{dt}$

= particle shrinkage rate

Substituting Eq. 3.3.3 in Eq. 3.3.1 and integrating over all sizes in the bed gives

$$
F_o - F_1 - F_2 = - \int_{\text{all R}} \frac{3WP_b(R) \, \mathscr{R}(R) \, dR}{R} \quad \ldots\ldots\ldots (3.3.4)
$$

Now making the population balance on the particles in a size range of R to R $-\Delta$R. In unit time we then have

$$
\begin{pmatrix} \text{solids} \\ \text{entering} \\ \text{feed} \end{pmatrix} - \begin{pmatrix} \text{solids} \\ \text{leaving in} \\ \text{overflow} \end{pmatrix} - \begin{pmatrix} \text{solids} \\ \text{leaving in} \\ \text{elutriation} \end{pmatrix} + \begin{pmatrix} \text{solids shrinking} \\ \text{into the interval} \\ \text{from the larger} \\ \text{size} \end{pmatrix}
$$

$$
- \begin{pmatrix} \text{solid shrinking} \\ \text{out of the} \\ \text{interval to a} \\ \text{smaller size} \end{pmatrix} + \begin{pmatrix} \text{solid combusted} \\ \text{due to shrinking} \\ \text{within interval} \end{pmatrix} = 0 \dots \dots (3.3.5)
$$

Then with the rate of carbon combustion term given by Eq 3.3.3, Eq. 3.3.5 becomes in symbols

$$
F_0 P_0(\bar{R}) \Delta R - F_1 P_1(\bar{R}) \Delta R - F_2 P_2(\bar{R}) \Delta R + WP_b(R) \cdot \left(\frac{dR}{dt}\right)\bigg|_R - WP_b(R) \cdot \left(\frac{dR}{dt}\right)\bigg|_{R-\Delta R}
$$

$$
+ \frac{3WP_b}{R}(\bar{R}) \left(\frac{dR}{dt}\right) \Delta R = 0 \quad \dots \dots (3.3.6)
$$

where $P_1(\bar{R})$ = overflow size distribution of particles in the size interval R to R $-\Delta$R

$P_2(\bar{R})$ = elutriation size distribution of particles in the size interval R to R $-\Delta$R

The rate of elutriation of solids of size R from a mixture is characterized by the net upward flux of this size of solid and is proportional to the weight fraction of bed consisting of size R. The equation is given

$$F_2 P_2 (\bar{R}) \Delta R = \mathcal{H}(\bar{R}) WP_b (\bar{R}) \Delta R \qquad \ldots\ldots(3.3.7)$$

where $\mathcal{H}(\bar{R})$ = elutriation constant of particles in the size interval R to R $-\Delta$R

Substituling Eq. 3.3.7 in Eq. 3.3.6, dividing Eq. 3.3.6 by ΔR, taking limits as ΔR $\longrightarrow$ O, and using the assumption of good mixing of solids in the bed that provides $P_b (R)$ = $P_1 (R)$, gives the general differential equation for fluidized bed with shrinking particles and with elutriation.

$$F_o P_o (R) - F_1 P_1 (R) - W\mathcal{H}(R) P_1 (R) - W \frac{d}{dR} (P_1 (R) \mathcal{R}(R)) + \frac{3WP_1 (R) \mathcal{R}(R)}{R}$$

$$= 0 \qquad \ldots\ldots(3.3.8)$$

In considering the size distributions of feed and overflow, the feed of one size and the size distribution of overflow from a single sizes feed is considered before. Then an inflow of wide size distribution is looked upon as a sum of single size feeds, and it is reasonable to expect the overflows to be the sum of overflows from the single side feeds. This is the procedure used

If feed solids are of size R_i, then for particle shrinkage the combustor and the overflow stream will both contain particles of size $\leqslant R_i$. Now for any size interval R to R-dR, not including the feed size R_i, Eq. 3.3.8 becomes

$$O - F_1 P_1(R) - W\mathcal{K}(R) P_1(R) - WP_1(R)\, \frac{d\mathcal{R}(R)}{dR} - W\mathcal{R}(R)\, \frac{dP_1(R)}{dR} + \frac{3W\mathcal{R}(R)P_1(R)}{R}$$

$$= 0$$

Rearranging gives

$$\frac{dP_1(R)}{dR} = \left[\frac{3}{R} - \frac{1}{\mathcal{R}(R)} \cdot \frac{d\mathcal{R}(R)}{dR} - \frac{F_1}{W\mathcal{R}(R)} - \frac{\mathcal{K}(R)}{\mathcal{R}(R)} \right] P_1(R) \quad \ldots\ldots(3.3.9)$$

Separating and integrating between R_i and R gives

$$\ln \frac{P_1(R)}{P_1(R_i)} = 3 \ln \frac{R}{R_i} - \ln \frac{R(R)}{R(R_i)} - \int_{R_i}^{R} \frac{F_1/W + \mathcal{K}(R)}{\mathcal{R}(R)}\, dR \quad \ldots\ldots(3.3.10)$$

Let us now evaluate $P_1(R_i)$. To do this take an interval R to $R - \Delta R$ with average radius $\bar{R}$ and including R_i. For shrinking solids no larges particles shrink into this interval, the fifth term in Eq. 3.3.6 is zero. Dividing by Δt and taking the limit for $\Delta R \rightarrow 0$, while keeping R_i in the interval gives

$$F_o - 0 - 0 + WP_b(R) \left. \frac{dR}{dt} \right|_R -0+0 \; = \; 0$$

or

$$P_1(R_i) \; = \; - \frac{F_o}{W \mathcal{R}(R)} \qquad\qquad \dots (3.3.11)$$

substituting Eq. 3.3.11 into Eq. 3.3.10 gives the size distribution of exit stream and the bed for shrinking particles:

$$P_1(R, R_i) \; = \; \frac{F_o}{W \left| \mathcal{R}(R) \right|} \cdot \frac{R^3}{R_i} \cdot I(R, R_i) \qquad\qquad \dots (3.3.12)$$

where

$P_1(R, R_i)$ = size distribution based on original feed of size R_i and the term $I(R, R_i)$ is defined as

$$I(R, R_i) \; = \; \exp \left[- \int_{R_i}^{R} \frac{F_1 W + \mathcal{K}(R)}{(R)} \; dR \right] \qquad\qquad \dots (3.3.13)$$

Now we are considering the feed of wide size distribution as a sum of single size feeds. Since the overflow size distribution of a single size feed has already been found (Eq. 3.3.12), the procedure for treating the feed of wide size distribution is straightforward in principle.

Now for shrinking particles, the particles leaving of a particular size R consist of particles originally of a variety of larger sizes. In term of size distributions,

$$\begin{pmatrix} \text{fraction of} \\ \text{overflow stream} \\ \text{of size R} \end{pmatrix} = \sum_{\substack{\text{all feed particles} \\ \text{of size not larger} \\ \text{than R}}} \begin{pmatrix} \text{traction of particles} \\ \text{overflowing which} \\ \text{are of size R and} \\ \text{which originally were} \\ \text{of size } R_i \end{pmatrix} \begin{pmatrix} \text{fraction} \\ \text{of size} \\ R_i \text{ in the} \\ \text{feed} \end{pmatrix}$$

in symbols this becomes

$$P_1(R) \quad R = \sum_{R_i=R}^{R_i=R_M} P_1(R,R_i)\, \Delta R . P_o(R_i)\, \Delta R_i \qquad \dots.(3.3.14)$$

where $P_1(R,R_i)\Delta R$ = fraction of particles overflowing which are of

size R and which originally were of size R_i

$P_o(R_i)\Delta R$ = fraction of size R_i in the feed

R_M = the largest size of particle in the feed.

Taking limits for R we find

$$P_1(R) = \int_{R_i = R}^{R_i = R_M} P_1(R,R_i)\, P_o(R_i)\, dR_i \qquad \dots.(3.3.15)$$

This expression relates the size distribution of exist stream $P_1(R)$ with that of the incoming stream $P_o(R)$ and the output distribution for entering size $R_i, P_1(R,R_i)$, which is given by Eq. 3.3.12
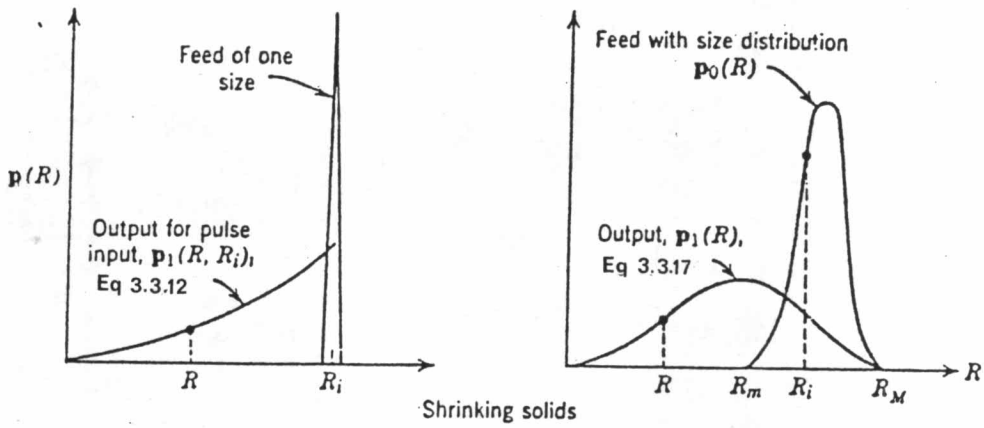
This relationship is shown in Figure 3.4

Fig. 3.4   Relation Between Size Distribution of Feed and Outflow
Streams, and Notation Used

Now substituting $P_1(R,R_i)$ by Eq. 3.3.12 gives

$$P_1(R) = \int_{R_i=R}^{R_i=R_M} \frac{F_o}{W\left|\mathcal{R}(R)\right|} - \frac{R^3}{R_i^3} \cdot I(R,R_i) - P_o(R_i)\ dR_i \qquad \ldots (3.3.16)$$

or in more useful form, the size distribution for shrinking
particles is given by

$$P_1(R) = \frac{F_o R^3}{W\left|\mathcal{R}(R)\right|} \cdot I(R, R_M) \int_{R_i=R}^{R_i=R_M} \frac{P_o(R_i)\,dR_i}{R_i^3 I(R_i, R_M)} \qquad \dots (3.3.17)$$

where I is defined in Eq. 2.3.13 and R_M is the largest size of feed. Integrating $P_1(R)$ over all particle sizes in the bed, thus from R_M to $R_{t \to \infty}$ for shrinking particles gives

$$\int_{R_t}^{R_M} P_1(R)\,dR = \int_{R_{t\to\infty}}^{R_M} \frac{F_o R^3 I(R, R_M)}{W\left|\mathcal{R}(R)\right|}\,dR \int_{R_i=R}^{R_M} \frac{P_o(R_i)\,dR_i}{R_i^3 I(R_i, R_M)}$$

$$1 = \frac{F_o}{W} \int_{R_{t\to\infty}}^{R_M} \frac{R^3 I(R, R_M)}{W\left|\mathcal{R}(R)\right|}\,dR \int_{R_i=R}^{R_i=R_M} \frac{P_o(R_i)\,dR_i}{R_i^3 I(R_i, R_M)}$$

$$\frac{W}{F_o} = \int_{R_{t\to\infty}}^{R_M} \frac{R^3}{\left|\mathcal{R}(R)\right|} \cdot I(R, R_M)\,dR \int_{R_i=R}^{R_i=R_M} \frac{P_o(R_i)\,dR_i}{R_i^3 I(R_i, R_M)} \qquad \dots (3.3.18)$$

We can see that $\dfrac{W}{F_o}$ term is the average residence time of burning char particles in the bed.

The equation for elutriation particles size distribution can be rearranged from Eq. (3.3.7)

$$P_2(R) = \frac{\mathcal{K}(R) W P_1(R)}{F_2} \qquad \dots (3.3.19)$$

Again the method for finding the outflow quantities is similar to the simpler special cases, though more tedious

1. First make a tabulation of values for the integral $I(R,R_M)$, hence $I(R_i,R_M)$, for suitable increment of R

2. Using these values in Eq. 3.3.18, find F_o, F_1 or W, whichever is unknown. If F_o is unknown, the solution is direct; however, finding F, or W requires adjusting guessed values of F_1 or W until Eq. 3.3.18 is satisfied.

3. Find $P_1(R)$ at selected R values by direct substitution in Eq. 3.3.15

4. Find F_2 from Eq. 3.3.4

5. Find $P_2(R)$ from Eq. 3.3.19

These equations above can be solved, if the values of elutriation constant, $\mathcal{K}(R)$, and the shrinking rate, $\mathcal{R}(R)$, of burning char in the bed are known. They both vary with the size of burning char particles. Several different equations including factors involving the elutriation rate constant and shrinking rate, were given separately in the literature. They are summarized and reviewed here.

3.4 Literature Review

3.4.1 Elutriation Constant

Elutriation refers to the selective removal of fines by entrainment from a bed consisting of a mixture of particle sizes.

The rate of elutriation of solids of size d_p from a mixture is characterized by the net upward flux of this size of solid

$$\left(\begin{array}{l} \text{rate of removal of solids} \\ \text{of size } d_p \text{ per area of bed} \\ \text{surface} \end{array} \right) = K^* \left(\begin{array}{l} \text{fraction of bed} \\ \text{consisting of} \\ \text{size } d_p \end{array} \right)$$

$$-\frac{1}{A_t} \frac{dW(d_p)}{dt} = K^* \frac{W(d_p)}{W} \qquad\qquad \ldots\ldots (3.4.1)$$

where

A_t = cross section area of bed

$W(d_p)$ = the weight of particles of size d_p

W = total weight of particles in bed

K^* = elutriation constant

In a mixture K^* varies with size of solids; a large value for K^* corresponds to a rapid removal rate, and $K^* = 0$ means that that particular size of particle is not removed at all by entrainment

The elutriation rate is also defined by

$$\left(\begin{array}{l} \text{rate of removal} \\ \text{of solids of size } d_p \end{array} \right) = \mathcal{K} \left(\begin{array}{l} \text{Weight of that size} \\ \text{solid in the bed} \end{array} \right)$$

or

$$-\frac{dW(d_p)}{dt} = \mathcal{K}\, W(d_p) \qquad \ldots(3.4.2)$$

In comparing definitions we see that

$$K^* = \frac{\mathcal{K}\, W}{A_t} \qquad \ldots(3.4.3)$$

Although $\mathcal{K}$ is also called an elutriation constant, we should note that it varies proportionaly with bed cross section and inversely with bed height. Also, in batch or unsteady-state experimentation $\mathcal{K}$ should change during a run as meterial is elutriated from the bed (W changes). The constant K^* is unaffected by these changes as long as the quality of fluidization remains the same.

Experimental data on attrition and elutriation rates obtained in both batch and continuous fluidized bed reactors have been correlated by several investigators, such as:

Tanaka, et al [13]

$$\frac{K^*}{\rho_g(U_o-U_t)} = 0.05\left(\frac{U_t\rho_g d_p}{\mu}\right)^{0.3}\left(\frac{(U_o-U_t)^2}{g\,d_p}\right)^{0.5}\left(\frac{\rho_s-\rho_g}{\rho_g}\right)^{0.15} \qquad \ldots(3.4.4)$$

Yagi and Aochi [14]

$$\frac{K^*d_p}{\mu}\cdot\frac{1}{Fr} = 0.0015Re_p^{0.6}+0.01\,Re_p^{1.2} \qquad \ldots(3.4.5)$$

where U_o = superficial velocity

U_t = terminal velocity of particle of size d_p

ρ_g = density of gas

μ = viscosity of gas

ρ_s = particle density

$\mathbf{Re}_p$ = Reynolds number = $\dfrac{U_t \, \rho_g \, d_p}{\mu}$ $\qquad$ ...(3.4.6)

$\mathbf{Fr}$ = Froude number = $\dfrac{(U_o - U_t)^2}{g \, d_p}$ $\qquad$ ...(3.4.7)

g = gravitational acceleration

These correlations were developed for solids other than coal char, limestone, and coal ash except for the Merrick and Highley (1974) as well Wen and Hashinger (1960) correlations.

The correlation of Wen and Hashinger[15] is

$$K^*(d_p) \propto (U_o - U_t) \left(\frac{(U_o - U_t)^2}{g \, d_p} \right)^{0.5} \cdot \left(\frac{d_p \rho_g U_t}{\mu} \right)^{0.725} \cdot$$

$$\left(\frac{\rho_s - \rho_g}{\rho} \right)^{1.15} \qquad \qquad ...(3.4.8)$$

$$\frac{K^*}{\rho_g(U_o-U_t)} = 1.7 \times 10^{-5}\left(\frac{(U_o-U_t)^2}{g\,d_p}\right)^{0.5} \cdot \left(\frac{d_p U_t \rho_g}{\mu}\right)^{0.725} \cdot$$

$$\left(\frac{\rho_s-\rho_g}{\rho_g}\right)^{1.15}\left(\frac{U_o-U_t}{U_t}\right)^{0.10} \qquad \qquad \ldots(3.4.9)$$

However, the correlation predicts no elutriation of particles larger than size d_{pt}, particle size with terminal velocity equal this is incorrect, and it is even less acculate for very fine particles since, assuming U_t is proportional to d_p^2, the correlation predicts that K^* reduces to zero as the particle size tends to zero. Hence a new form of correlation was required.

The Merrick and Highley correlation[16] is such a correlation.

$$\frac{K^*}{\rho_g U_o} = A + 130\ \exp\left[-10.4\ \left(\frac{U_t}{U_o}\right)^{0.5}\left(\frac{U_{mf}}{U_o-U_{mf}}\right)^{0.25}\right] \qquad \ldots(3.4.10)$$

$$\text{or } \mathcal{K} = \frac{\rho_g U_o A_t}{W}\left[A+130\ \exp\left[-10.4\left(\frac{U_t}{U_o}\right)^{0.5}\left(\frac{U_{mf}}{U_o-U_{mf}}\right)^{0.25}\right]\right] \qquad \ldots(3.4.11)$$

A = 0.0001 for the 36 inch combustor with 13 ft. freeboard

A = 0.0015 for the BCURA combustor with 6 ft freeboard

Merrick and Highley compared their correlation with that of Wen and Hashinger by calculating elutriation rate constants for a wide range of operating parameters using both correlations. In general, the agreement was good for particle sizes intermediate between zero and d_{pt}, but, for reasons discussed previously, the predictions differed considerably for very fine particles and for particles of about d_{pt} and larger.

There is another simple correlation proposed by Colakyan, et al., for calculating elutriation constant. This correlation is applied to the bed that the freeboard exceeds the transport disengaging hight (TDH), and to the large beds with large particles and high gas velocities.

The simple form of the correlation of Colakyan et. al[17] is

$$K^* = K. \left(1 - \frac{U_t}{U_o}\right)^n \qquad \qquad \ldots (3.4.12)$$

where $\qquad\qquad$ K = a constant

$\qquad\qquad\qquad\qquad$ n = an exponent

For the runs made without the immersed tube array, a relationship of the following form was obtained:

$$K^* = 33.9 \left(1 - \frac{U_t}{U_o}\right)^2 \qquad \qquad \ldots (3.4.13)$$

Similar forms were obtained for the runs made with the tube bundle positioned 25 cm above the distribution plate

$$K^* = 33.3 \left(1 - \frac{U_t}{U_o}\right)^2 \qquad \dots (3.4.14)$$

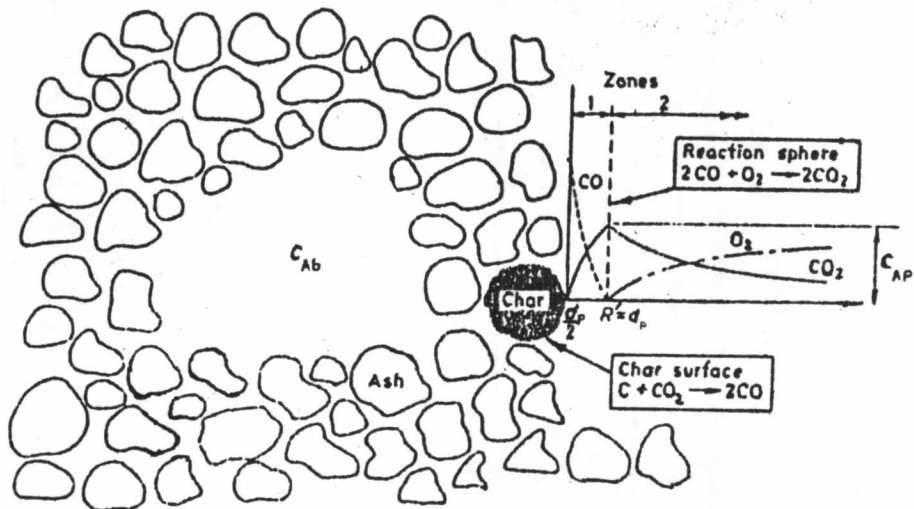### 3.4.2 Oxygen Transfer Rate to One Particle[18]

Fig. 3.5 Char Particle Burning in Particulate Phase
of a Fluidized Bed

The shrinking rate of burning char particle in the bed is considered from the combustion rate of a coal particle or the oxygen rate to one particle.

The mechanism of combustion of the fixed carbon in the coal is an important thing to be considered. The assumptions are

(1) Coal loses its volatile content almost instantaneously on entering bed, the combustion of remaining carbon is considered.

(2) The fixed carbon reaction is very fast, this leads to diffusion resistance control not kinetic reaction control (Field[19] has presented that the combustion of coal is kinetic controlled for small particle of size less than 50 μm, the transition from kinetic to diffusion control taking place over the particle size range 50 μm to 100 μm, for the particle greater than 100 μm combustion is diffusion controlled)

(3) Fig. 3.5 shows a char particle with its surrounding ash particles agitated by rising bubbles containing most of the oxygen. Thus there is a diffusional resistance between the bubbles where the oxygen concentration is C_{Ab} and the ash phase where the concentration is C_{Ap}. There are also local concentration gradients around each char particle as indicated in Fig.3.5 . These concentration gradients are a logical consequence of assuming fast reactions leading to what has been termed the "two-film theory."

The reaction sphere is at d_p from the surface of the particle. Carbon monoxide produced at the surface diffuses towards the reaction zone from the particle side, and O_2 diffuses in from the main stream and they burn in a diffusion flame to produce CO_2. From the stoichiometry, one half of the CO_2 diffuses back to the particle surface to be reduced to CO and the other half diffuses out into the main stream. Existence of reaction zones around carbon particles is quite apparent from the characteristic blue halo, and from the fact that no CO appears in the main stream when these is an abundant supply of O_2.

Mass transfer is primarily due to molecular diffusion, and assuming that the concentration profiles are established quickly as the particle shrinks, we have

$$\frac{d}{dr} (r^2 \frac{dc}{dr}) = 0 \qquad \dots (3.4.15)$$

where C = molar concentration

r = radial distance

The boundary conditions are as follow:

$$r = \frac{d_p}{2} \quad , \quad Cco_2 = 0$$

$$r = R' = d_p \, , \quad Cco = Co_2 = 0$$

$$r \longrightarrow \infty \quad , \quad Cco_2 = 0, \quad Co_2 = C_{AP}$$

where R' = radius of the reaction sphere assumed that $R' = d_p$ and from stoichiometry and continuity at reaction sphere, R'

$$-\tfrac{1}{2} (\frac{dCco}{dr}) = (\frac{dCco}{dr})_1 = - (\frac{dCco}{dr})_2 = (\frac{dC_o 2}{dr})_2 \quad \dots (3.4.16)$$

So we get

in zone 1: $Cco = 2 C_{Ap} (\frac{d_p}{r} - 1)$

$$Cco_2 = C_{Ap} (2 - \frac{d_p}{r})$$

in zone 2:
$$Cco_2 = \frac{C_{Ap}\, d_p}{r}$$

$$Co_2 = C_{Ap}(1 - \frac{d_p}{r})$$

where C_{Ap} is the concentration of O_2 in the particulate phase

At $r = R' = d_p$, the molar flow of O_2 to a particle, n, is

$$n = 4\pi R^2 E \left(\frac{dCo_2}{dr}\right)_R = 4\pi d_p\, EC_{Ap} \qquad \ldots(3.4.17)$$

where E is the effective diffusion coefficient or dispersion coefficient for mass transfer through the gas within the ash phase. The value of E is less than the molecular diffusion coefficient, D_A, because of the ash particles, and the ratio E/D_A depends upon the porosity and tortuosity of the ash phase.

The transfer rate given by equation (3.4.17) may be compared with the transfer rate that would occur with no chemical reaction, other than at the particle surface. From equation (3.4.15) with boundary conditions

$$r = dp/2 , \quad Co_2 = 0$$

$$Co_2 = C_{Ap}$$

$$n_o = 2\pi d_p\, EC_{Ap} \qquad \ldots(3.4.18)$$

or
$$n_o = K_g\, \pi\, d_p^2\, C_{Ap} \qquad \ldots(3.4.19)$$

where n_o = oxygen transfer rate without gas phase reaction

K_g = mass transfer coefficient

$K_g = 2E/d_p$ ....(3.4.20)

$\therefore \quad Sh \quad = K_g d_p/D_A$ ....(3.4.21)

$\therefore \quad Sh \quad = 2E/D_A$ ....(3.4.22)

Equation (3.4.17) may be rewriten as

$n \quad = \quad 2\pi Sh D_A d_p C_{Ap}$ ....(3.4.23)

or $= 2\pi R' Sh\ D_A C_{Ap}$ ....(3.4.24)

where $R' = d_p$

This equation will be used to calculate the rate of combustion throughout the life of a char particle with constant sherwood number, Sh.

The values of the Sherwood number,Sh, and concentration of oxygen in the particulate phase are the continuing factors to be derived.

3.4.3 Sherwood Number (Sh)[20]

The value of Sh depends on the ash voidage fraction, the turtuosity of the voids between the ash particles, and the ratio of the diameters of the char and ash particles.   In spite of the

possible variation of Sh during an experiment as the char burns down to zero, the Sh is assumed to be constant at the particular size of burning char size distribution in the bed. However Sh varies with the different size of burning char size distribution in the bed.

The particle sherwood number is an important factor delivering oxygen from the particulate phase to the particle surface.

From dimensional analysis

$$k_{mA} = \psi (D_A, d_p, G, \mu)$$

where

k_{mA} = individual mass transfer coefficient

G = mass velocity

μ = viscosity of gas

$$\frac{k_{mA} \rho_g}{G} = \psi_1 \left(\frac{d_p G}{\mu} , \frac{\mu}{D_A \rho_g} \right)$$

multiply by $(d_p G/\mu)(\mu/D_A \rho_g)$

$$\frac{k_{mA} d_p}{D_A} = \psi_2 \left(\frac{d_p G}{\mu} , \frac{\mu}{D_A \rho_g} \right)$$

$$\frac{k_{mA} d_p}{D_A} = \text{Sherwood number of particle} = Sh$$

$$\frac{d_p G}{\mu} = \frac{d_p v \, \rho_g}{\mu} = \text{Reynolds number} = \text{Re}$$

where v is the gas velocity

$$\frac{\mu}{D_A \rho_g} = \text{Schmidt number} = \text{Sc}$$

$$\text{Sh} = \psi_2 (\text{Re, Sc})$$

From Fig. 3.6. The line in the figure approaches an asymptote of Sh = 2.0 at low values of $(\text{Re})^{1/2} (\text{Sc})^{2/3}$. The line is represented by the equation

$$\text{Sh} = 2 + 0.6 \, (\text{Re})^{\frac{1}{2}} \, (\text{Sc})^{1/3} \qquad \ldots (3.4.25)$$

$$\text{Sh} = 2 \pm 0.6 \left(\frac{d_p U_o \rho_g}{\mu} \right)^{\frac{1}{2}} \left(\frac{\mu}{\rho_g D_A} \right)^{1/3}$$

This is a single sphere particle correlation of sherwood number that relates to the Reynolds and Schmidt numbers. This correlation is expected to be used with small particle interaction in the bed.
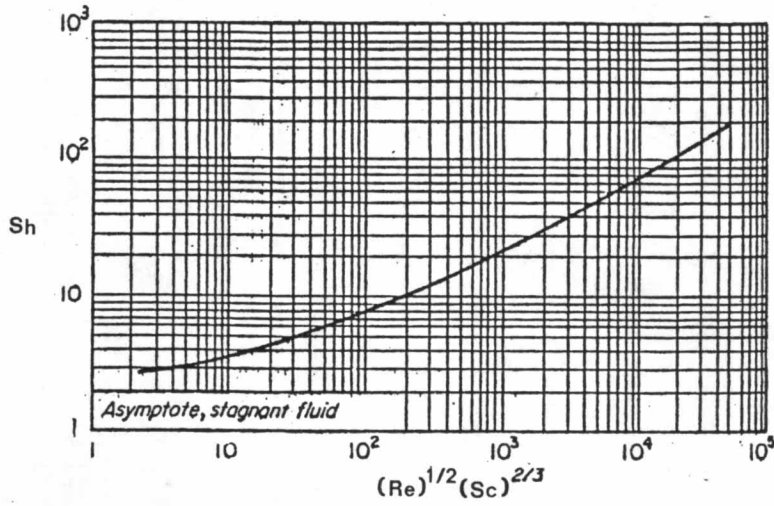
Figure 3.6 Heat and Mass Transfer, Flow Past Single Sphere[20]

3.4.4 Concentration of Oxygen in Particulate Phase (C_{Ap})[21]

From Eq.3.4.24, in order to detemine the shrinking rate of coal particle,

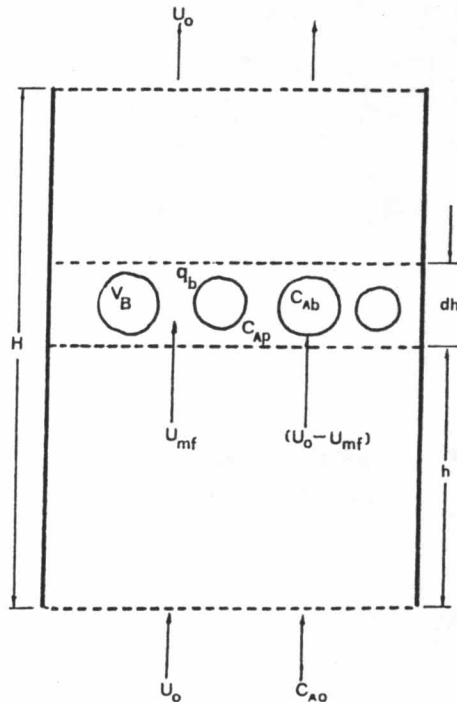we have to know the concentration of oxygen in the particulate phase.

Fig. 3.7 Bubble Model: Concentrations and Flows.

From Fig. 3.7 a material balance over the bubble phase in this element dh, yields,

$$Ndh \ q_b \ (C_{Ap} - C_{Ab}) = Ndh \ V_B \ \frac{dC_{Ab}}{dt} = Ndh \ V_B U_b \ \frac{dC_{Ab}}{dh}$$

$$C_{Ab} - C_{Ap} = - \frac{V_b U_b}{q_b} \cdot \frac{dC_{Ab}}{dh} \qquad \qquad \ldots (3.4.26)$$

N = number of bubble /unit bed volume

q_b = interphase gas-exchange rate between bubble and particulate phase

C_{Ap} = gas concentration of A, oxygen, in the particulate phase

C_{Ab} = gas concentration of A, oxygen, in the bubble phase

h = height of bubble above distributor

V_B = volume of a bubble

Boundary Condition: $C_{Ab} = C_{Ao}$ when h = 0

Assumption

    1) bubble size is uniform at a certain U_o

    2) C_{Ap} is constant at a certain U_o because of back mixing

    3) C_{Ab} varies with the height of bubble

$$- \int_0^H \frac{q_b}{V_b U_b} \, dh = \int_{C_{Ao}}^{C_{Ab}} \frac{dC_{Ab}}{C_{Ab} - C_{Ap}}$$

$$C_{Ab} = C_{Ap} + (C_{Ao} - C_{Ap}) \exp\left(- \frac{q_b H}{V_B}\right)$$

$$C_{Ap} = \frac{C_{Ab} - C_{Ao} \exp(-X_b)}{1 - \exp(-X_b)} \qquad\qquad \dots(3.4.27)$$

$$\frac{q_b H}{V_b U_b} = \frac{(K_{bp})_b \, H}{U_b} = X_b \qquad\qquad \dots(3.4.28)$$

where $(K_{bp})_b$ = the interchange coefficient between bubble and

particulate phase

H = bed height

C_{Ap} is constant all over the bed, it does not vary with height of the bubble rising in the bed, but it changes depending on the value of X_b, even though the height of the bed, H, is constant.

Consequently the value of X_b is an important factor relating to delivery of oxygen from the bubble to the particulate phase. X_b is the number of times that a bubble is flushed out-by through-flow and diffusion-in passing through the bed.

X_b will be changed if $(K_{bp})_b$ or U_b is changed, despite of fixed height of bed. And $(K_{bp})_b$ and U_b vary with average bubble diameter (d_b), and the average bubble diameter varies with superficial velocity, U_o.

The $(K_{bp})_b$, U_b, d_b, U_{mf}, will be presented respectively. All of these mechanical values relate to the bed material which is mainly limestone particles(more than 99 % of particles in the bed).

3.4.5 Gas Interchange Coefficient between bubble and particulate phase $(K_{bp})_b$

A number of correlations have been developed to predict gas interchange rates between bubble and phase in fluidized beds. Several of these correlations have been evaluated to determine their applicability to fluidized bed combustors. The Davidson and Harrison correlation has been chosen for use in this model. Kunii and Levenspiel suggest that this expression actually predicts exchange rates between bubble and cloud.In the fluidized bed combustorif the superficial gas velocity is high, the bubbles will be large and the bubble clouds will be thin. The bubble clouds overlap each other and seem to be the particulate phase. Hence the two phases model of bubble phase and particulate phase is considered. In combustion, oxygen in the air will transfer from bubble phase to particulate phase by both convection and diffusion mechanisms.[10,22]

total mass transfer = mass transfer by convection + mass transfer by diffusion from bubble to particulate phase

$$- \frac{dN_{Ab}}{dt} = -S_{bp}K_{bp}(C_{Ab}-C_{Ap}) - (qC_{Ab}-qC_{Ap})$$

$$= -(S_{bp}K_{bp}+q)(C_{Ab}-C_{Ap}) \qquad \qquad \dots(3.4.29)$$

N_{Ab} = the mass of gas A transfered from bubble phase to particulate phase

S_{bp} = surface area perpendicular to mass flow from bubble to particulate phase

K_{bp} = mass transfer coefficient

q = volumetric gas flow (convection) into and out of a single bubble

= gas velocity into and out of bubble x cross section area of bubble

$$q = 3U_{mf} \cdot \pi R_b^2 = \frac{3\pi}{4} U_{mf} d_b^2 \qquad \ldots (3.4.30)$$

Davidson and Harrison found that

$$k_{bp} = 0.975 \, D_A^{\frac{1}{2}} \left(\frac{g}{d_b}\right)^{1/4}$$

$$\therefore -\frac{1}{V_b}\frac{dN_{Ab}}{dt} = \frac{-1}{V_b}\left(\frac{3}{4}\pi U_{mf} d_b^2 + 0.975 \, D_A^{\frac{1}{2}}\left(\frac{g}{d_b}\right)^{\frac{1}{4}}\pi d_b^2\right)(C_{Ab}-C_{Ap})$$

$$= -(K_{bp})_b (C_{Ab}-C_{Ap}) \qquad \ldots (3.4.31)$$

where $(K_{bp})_b = 4.5 \, \dfrac{U_{mf}}{d_b} + 5.85 \, \dfrac{D_A^{\frac{1}{2}} g^{\frac{1}{2}}}{d_b^{5/4}} \qquad \ldots (3.4.32)$

3.4.6 Bubble Diameter (d_b)

Various correlations for estimating bubble diameters in fluidized beds have appeared in the literature. The correlations in

Table 3.1 are derived from data obtained from relatively small diameter
beds (often 10cm in diameter).

Table 3.1 Summary of Correlations for Bubble Diameters in
Fluidized Beds [23]

Yasui et al (1958) $\quad d_b = 1.6 \quad d_p \left(\dfrac{U_o}{U_{mf}} - 1\right)^{0.63} .h$

Kato and Wen (1969) $\quad d_b = 1.4 \quad d_p \left(\dfrac{U_o}{U_{mf}}\right) h + D'_{Bo}$

Park et al (1969) $\quad d_b = 33.3 \ d_p^{1.5} \quad \left(\dfrac{U_o}{U_{mf}} - 1\right)^{0.77}$

Whitehead et al (1967) $\quad d_b = 9.76 . \left(\dfrac{U_o}{U_{mf}}\right)^{0.33} (0.032h)^{.054}$

Rowe at el (1972) $\quad d_b = -A + Bh + C \left(\dfrac{U_o}{U_{mf}}\right)$

$$+ Dh \left(\dfrac{U_o}{U_{mf}}\right) + E \left(\dfrac{U_o}{U_{mf}}\right)^2$$

Geldart (1971) $\quad d_b = D'_{Bo} + 0.027 \ (U_o - U_{mf})^{0.94}$

Chiba et al (1973) $\quad d_b = D''_{Bo} \ (2^{7/6} - 1) \ (h - h_{Bo})/$

$$(D''_{Bo} + 1)^{2/7} \text{ for } h < h_k$$

where $\qquad D'_{Bo} \quad = \quad (6 \ G/\pi)^{0.4}/ \ g^{0.2}$

$\qquad\qquad D_{Bo} \quad = \quad (6 \ G/\pi \ K_B^{0.4}/ \ g^{0.2}$

A,B,C,D,E,K_b $\quad = \quad$ constants determined by the properties of the solid particles

$\qquad\qquad h_{Bo} \quad = \quad$ height of jet above the distributor

$\qquad\qquad h_K \quad = \quad$ height when the buble radius becomes equal to the hole distributor pitch

$\qquad\qquad G \quad = \quad$ Volumetric gas flow rate through a nozzle

But they are not useful in predicting the change in the bubble diameter when the bed diameter is changed.

Mori and Wen[23] proposed a correlation by considering the effect of bed diameter on bubble diameter. The correlation is

$$\frac{d_{bM} - d_b}{d_{bM} - d_{bo}} = \exp(-0.3h/D_t) \qquad \ldots.(3.4.33)$$

where d_{bo} = initial bubble diameter at the distributor

$$= 0.347 \left(A_t \ (U_o - U_{mf})/n_d \right)^{2/5} \quad \text{for perforated plate}$$
$$\ldots.(3.4.34)$$

n_d = number of orifice openings in the distributor

d_{bM} = maximum bubble diameter due to total coalescences of bubbles

h = elevation above distributor

D_t = diameter of fluidized bed

This correlation is fairly acculate in predicting bubble diameter especially for the following variable ranges:

$$30 < D_t < 130 \text{ cm}$$

$$0.5 < U_{mf} < 20 \text{ cm/s}$$

$$0.006 < d_p < 0.045 \text{ cm}$$

$$U_o - U_{mf} < 48 \text{ cm /s}$$

where U_{mf} = minimum fluidizing velocity

U_o = superficial velocity

However the correlation in Table 3.1 and Eq. 3.4.33 are used for fine particles bed. The correlation for predicting bubble diameter in large particles fluidized bed was proposed by Cranfield and Geldart.[24] The large particles that they used in the experiment are 1000-2000 μ m. This correlation is

$$d_b = 0.0326 \ (U_o - U_{mf})^{1.11} \ h^{0.81} \pm 10 \ \% \qquad \ldots (3.4.35)$$

There is no distributor term in the above correlation since bubbles do not originate at the distributor and it is therefore prudent to limit its use to conditions when $h > 5$ cm

3.4.7 Bubble Velocity[21,25]

If the gas velocity is suddenly raised from U_{mf} to U_o a crowd of bubbles will begin to rise through the bed, and, in addition, the section of bed ahead of this crowd will itself move upward with velocity $(U_o - U_{mf})$. Thus every bubble meets a rising bed ahead. If the relative velocity between bubble and emulsion is unaffected by

the interaction between neighboring bubbles, then this velocity should be given by the rise velocity U_{br} of single bubbles in beds at minimum fluidizing conditions. With this approximation the absolute rise velocity of bubbles in bubbling beds is given by

$$U_b = U_o - U_{mf} + U_{br} \qquad \qquad \ldots \ldots (3.4.36)$$

From the correlation of Cranfield and Geldart, the correlation of bubble rise velocity for large particle is given by

$$U_{br} = 0.711(gd_b)^{\frac{1}{2}}$$

From Eq. 3.4.28, $X_b = \dfrac{(K_{bP})_b^{H}}{U_b}$, the term $\dfrac{H}{U_b}$ is the residence time of bubble in the bed. The value of X_b, the number of transfer units increases as the bubble residence time in the bed decreaes.

3.4.8 Minimum Fluidization Velocity (U_{mf})

Minimum fluidization velocity is one of the important parameters in the design and operation of fluidized bed reactors. Many papers suggesting a numbers of equations for predicting minimum fluidization velocity have been published such as equations shown in Table 3.2

26

Table 3.2 Equations Used to Predict the Minimum Fluidization Velocity

Equation	Range of applicability	No. of equation	Author
$Ga = 150 \dfrac{1 - \epsilon_{mf}}{\psi^2 \epsilon_{mf}^3} Re_{mf} + 1.75 \dfrac{Re_{mf}^2}{\psi \epsilon_{mf}^3}$	Not limited	5	Ergun (1952)
$u_{mf} = \dfrac{(\psi \cdot d_p)^2}{150} \dfrac{\rho_S - \rho_g}{\mu} g \dfrac{\epsilon_{mf}^3}{1 - \epsilon_{mf}}$	Small particles $Re_{mf} < 20$	6	Kunii and Levenspiel (1969)
$u_{mf}^2 = \dfrac{\psi d_p}{1.75} \dfrac{\rho_S - \rho_g}{\rho_g} g \epsilon_{mf}^3$	Large particles $Re_{mf} > 1000$	6	Kunii and Levenspiel (1969)
$G_{mf} = \dfrac{0.005(\psi \cdot d_p)^2}{\mu_F (1 - \epsilon_{mf})} g \rho_g (\rho_S - \rho_g) \epsilon_{mf}^3$	$Re_{mf} < 10$	7	Leva (1959)
$G_{mf} = \dfrac{(\psi \cdot d_p)^2 g}{18 \mu} (\rho_g - \rho_g) \rho_g \dfrac{\epsilon_{mf}^3}{1 + 0.5(1 - \epsilon_{mf})}$	$Re < 2$	8	Johnson (1949)
$G_{mf} = 0.171 \psi d_p \rho_g \left(\dfrac{\epsilon_{mf}}{1 - \epsilon_{mf}} \right)^3$ $\times \left(\dfrac{g^2 \rho_S \epsilon_{mf}}{\mu (1 - \epsilon_{mf})(1 + 0.5(1 - \epsilon_{mf}))} \right)^{1/3}$	$Re > 2$	9	Johnson (1949)
$Re_{mf} = \left(33.7^2 + 0.0408 \dfrac{d_p^3 \rho_f (\rho_S - \rho_g)g}{\mu^2} \right)^{0.50} - 33.7$	Not limited	10	Wen and Yu (1965)
$u_{mf} = \dfrac{d_p^2 (\rho_S - \rho_g)g}{1650 \mu}$	$Re < 20$ Small particles	10	Wen and Yu (1965)
$Re_{mf} = \dfrac{Ar}{1400 + 5.22 Ar^{0.50}}$	Not limited	11	Todes (1957)
$G_{mf} = \dfrac{0.00125 d_p^2 (\rho_S - \rho_g)^{0.90} \rho_g^{1.1} g}{\mu}$	Not limited	12	Miller and Logwinuk (1951)

$Re = u_G d_p \rho_g / \mu$, particle Reynolds number
$Re_{mf} = u_{mf} d_p \rho_g / \mu$, particle Reynolds number at
   fluidization velocity
$Ga = g d_p^3 \rho_f \cdot (\rho_S - \rho_g) / \mu^2$, Galilei number
$Ar = g d_p^3 \rho_g \cdot (\rho_S - \rho_g) / \mu^2$, Archimedes number

Pata and Hartman (1978)[26] used Ergun equation (1952)[27] to predict the minimum fluidization velocity of bed material, limestone, and the predicted values were in agreement with experimental data.

Ergun equation derivation can be seen in Appendix A

Sometimes the minimum fluidization velocity of binary mixture of different sized particles is considered. Agbin A.J., et al[28], carried out experiments and got several **data.** The data are in agreement with the following simple empirical expression

$$\frac{U_{mfc}}{U_{mfs}} = \left(\frac{U_{mfB}}{U_{mfs}}\right)^{X_B^2} \qquad \ldots(3.4.37)$$

where U_{mfB} = minimum fluidization velocity of larger particles

U_{mfs} = minimum fluidization velocity of smaller particles

U_{mfc} = minimum fluidization velocity of the mixture

X_B = fraction of larger particles

This expression can be used where the ratio of d_{ps}/d_{pB} is less than 0.3.

d_{ps} = diameter of smaller particle

d_{pB} = diameter of larger particle

3.4.9 Terminal Velocity

The velocity that can carry the fly-ash out at the particular burning char particle size is terminal velocity which effects the elutriation directly.

Kunii and Levenspiel (1969)[29] proposed the equations for calculating terminal velocity. The equations are

$$U_t, \text{ spherical } = \frac{g(\rho_s - \rho_g)d_p^2}{18\,\mu} \qquad \text{for } Re_p < 0.4 \dots (3.4.39)$$

$$U_t, \text{spherical } = \left(\frac{4}{225} \frac{(\rho_s - \rho_g)^2 g^2}{\rho_g \mu} \right)^{1/3} d_p \qquad \text{for } 0.4 < Re_p \quad 500 \dots (3.4.40)$$

$$U_t, \text{spherical} = \left(\frac{3.1g(\rho_s - \rho_g)dp}{\rho_g} \right)^{\frac{1}{2}} \qquad \text{for } 500 < Re_p < 2000,000$$

$$\dots (3.4.41)$$

The derivations of Eq. (3.4.39),(3.4.40),(3.4.41) are shown in Appendix B. These equations are only strictly applicable to spherical particles. Pettyjohn and Christiansen have proposed that the terminal velocity for non-spherical particles be estimated by multiplying the above values of U_t by correction factor,[25] where

where φ = sphericity of particle

$$\mathcal{G} = 0.843 \log \left(\frac{\varphi}{0.065} \right) \qquad \dots (3.4.42)$$

3.4.10 Carbon Residence time in bed

One of the most important factors that affects the overflow and the carbon loading is the carbon residence time. The average residence time of particles in bed is calculated by

$\bar{t}$ = the average residence time of particles in bed

$$\bar{t} = \frac{W}{F_O} \qquad \qquad \dots (3.4.43)$$

W = the weight of the carbon in bed while burning

F_O = the carbon feed rate

The term $\frac{W}{F_O}$ can be seen in Eq. 3.3.18. The value of W can be calculated by Eq. 3.3.18 if F_1, the carbon overflow rate, is known. The value of F_1 can be obtained from the experiment. In general the percent of carbon weight in bed while burning is between 1 % to 0.1 % of the weight of bed material. The simple equation for W is given

$$W = \text{percent of carbon burning in bed} \times W_B \qquad \dots (3.4.44)$$

where W_B = weight of bed material in the bed

The value of W_B can be calculated by the equations in next sections.

3.4.10 Bed Expansion (L_f/L_{mf}) and Bed Weight (W_B)

Babu et al (1978) have proposed a correlation for expanded bed height based on a comprehensive study of a number of earlier investigations. Most of the data on which the correlation is based is for small particles. The correlation is given by

$$\frac{L_f}{L_{mf}} = \frac{1 + 10.978 (U_o - U_{mf})^{0.738} d_p^{1.006} \rho_s^{0.376}}{U_{mf}^{0.937} \rho_g^{0.126}} \qquad \dots (3.4.45)$$

But the correlation used for large particles and high pressure is [30]

$$\frac{L_f}{L_{mf}} = 0.583 \, Re_x^{0.12} \left(\frac{L_{mf}}{d_t} \right)^{0.5} P_B^{-0.2} \qquad \dots (3.4.46)$$

where L_f = expanded bed height

L_{mf} = bed height at minimum fluidization

d_t = bed diameter

P_B = operating bed pressure

Re_x = Reynolds number based on excess gas velocity

$$Re_x = \rho_g \, (U_o - U_{mf}) \, d_p / \mu \qquad \dots (3.4.47)$$

This equation is applicable for $P_B \leqslant 5$ atm and $U/U_{mf} \leqslant 5$

Hence, for atmospheric pressure

$$\frac{L_f}{L_{mf}} = 0.583 \, Re_x^{0.12} \left(\frac{L_{mf}}{d_t} \right)^{0.5} \qquad \dots (3.4.48)$$

or $L_{mf} = (L_f / (0.583 \, Re_x^{0.12} \, d_t^{-0.5}))^{0.6667}$ $\quad\quad\quad$ .... (3.4.49)

The weight of bed material inside the bed is

$$W_B = L_{mf} \, A_t \, (1 - \epsilon_{mf}) \, \rho_s \quad\quad\quad\quad \dots (3.4.50)$$

where ϵ_{mf} = bed voidage at minimum fluidization

A_t = bed cross-section area

ρ_s = bed particle density

3.4.11 Particle Classification and Characterization

One parameter that effects the validity of the equations used is particle size.

Geldart[31] attempted to describe in details the hydrodynamic behavior of solid forming a bed when fluidized by gas. He classified solid particles into four characteristic groups in order to indentify the mode of fluidization according to the size and density of particles, as shown in Fig. 3.8
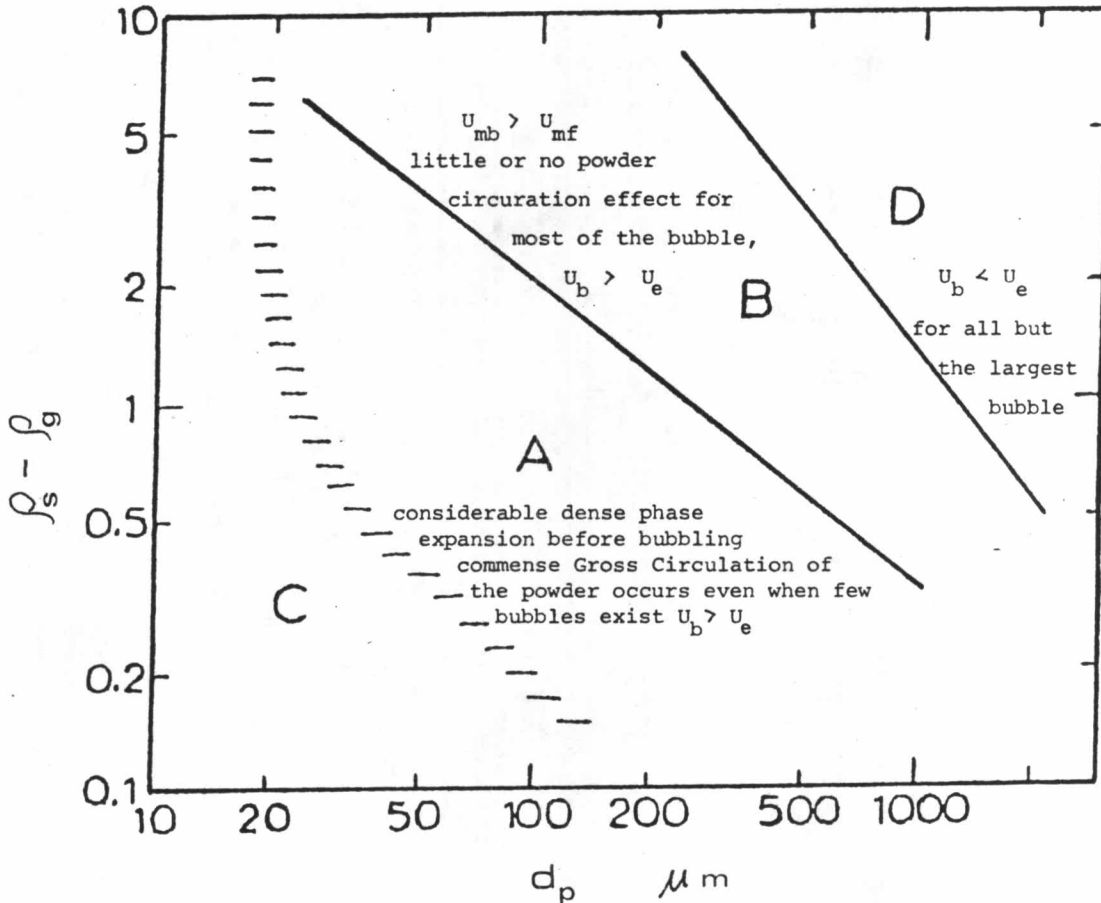

$U_{mb} > U_{mf}$
little or no powder
circuration effect for
most of the bubble,
$U_b > U_e$

B

D

$U_b < U_e$
for all but
the largest
bubble

A

considerable dense phase
expansion before bubbling
commense Gross Circulation of
the powder occurs even when few
bubbles exist $U_b > U_e$

C

Axis: $\rho_s - \rho_g$ vs d_p μm

Fig. 3.8 Four Groups of Particles Proposed By Geldard

These four groups are groups A,B,C and D. Particles belonging to group B and D are most typical of many applications of fluidization technology. Group B comprises of particles of mean diameter, d_p and density, ρ_s, lying in the ranges: $40 \mu m < \bar{d}_p < 500$ μm, and 1400 kg m$^3 < \rho_s < 4000$ Kg/m^3. Bubbles form in beds of such powders at or only slightly above U_{mf}. The majority of the bubbles rise faster than the interstitial gas velocity and bubble size increases linearly with bed height and excess gas velocity, $U-U_{mf}$. Bubble coalescence is the predominant phenomenon. Group D refers to powders whose particles are large in size and/or, very dense. In this case the majority of the bubbles

rise slower than the interstitial gas. The gas velocity in the dense phase is high and solids mixing is relatively poor. The flow regime around particles may be turbulent. The properties of powders belonging to this groups are not well understood at the present time due to the availability of only limited amount of experimental information on large particle fluidization behavior[32] and most of it is rather qualitative.[33]

The terms "small" and "large" particles used in the literature to signify particle size do not have any precise basis and very often they refer to groups B and D respectively. Bubble correlations based on group B or D particles should not be extended to other types without careful consideration of particles properties.[34]